Polymer 172 (2019) 126–132

Contents lists available at ScienceDirect

Polymer

journal homepage: www.elsevier.com/locate/polymer

Effect of ion concentration on the properties of polyisoprene-sodium styrene sulfonate elastomeric ionomers prepared by emulsion polymerization

Sarah E. Blosch[a], E. Bruce Orler[a,b], Samantha J. Talley[a,b], Robert B. Moore[a,b], S. Richard Turner[a,b,*]

[a] Macromolecules Innovation Institute, Virginia Tech, Blacksburg, VA, 24061-0344, USA
[b] Department of Chemistry, Virginia Tech, Blacksburg, VA, 24061-0344, USA

HIGHLIGHTS

- Copolymers of isoprene and sodium styrene sulfonate create ionomers with properties that change in relation to ion content.
- Large-scale aggregation was not shown in thermal properties, or small angle x-ray scattering.
- As ion concentration increased properties including stress relaxation, tensile, hysteresis, and adhesion improved.
- Property changes are due to chemical crosslinking and systematic increases in physical crosslinking with ion content.

ARTICLE INFO

Keywords:
Ionomer
Isoprene
Sulfonated styrene
Structure-property relationship

ABSTRACT

A series of isoprene and sodium styrene sulfonate copolymers (poly(I-*co*-NaSS)) was synthesized with systematically varied concentrations of ions using radical emulsion polymerization. Their chemical structures and morphologies were characterized and structure-mechanical relationships were determined. The SAXS scattering profiles and the thermal properties remained unchanged as ion content increased. In contrast, the toughness and stiffness of the copolymers increased and the adhesion strength was significantly improved as the ion content increased from 1.2 mol % to 4.6 mol % NaSS.

1. Introduction

Ionomers are used in many applications including adhesives, thermoplastic elastomers, rheology modifiers, etc. [1]. They are polymers containing less than 10 mol% of ionic groups, which exhibit properties dominated by intra- and intermolecular noncovalent interactions between ionic groups. Ions pairs tend to aggregate into triplets, quadruplets, and higher order aggregates comprised of many ion pairs, termed multiplets, consisting of an ion-rich domain encompassed by a region of restricted polymer chain mobility that exhibits its own glass transition [2]. The electrostatic interactions within the ion-rich domain of a multiplet are sufficiently strong to primarily determine ionomer morphological development, rather than elastic forces which oppose ionic aggregation. The strength of electrostatic interactions within ion-pairs is determined by the species of ionic functional group and the associated counter-ion group. Chain mobility is directly influenced by the strength of the electrostatic interactions, which affects mechanical properties, such as toughness, stiffness, and in the case of elastomers, the elasticity. The morphology of sulfonate ionomers is comprised of stronger ionic interactions than carboxylate ionomers [3], resulting in tunable physical properties related to the identity of the ionic moiety [4]. Sulfonate ionomers and carboxylate ionomers are commonly synthesized by functionalizing styrene units with metal sulfonates and metal carboxylates, respectively.

Isoprene copolymerized with low molar percentages of sodium styrene sulfonate (poly(I-*co*-NaSS)) has been investigated [5–11]. Previous investigations focused on the emulsion copolymerization, chemical characterization, and solubility, of isoprene with sodium styrene sulfonate [5–8], for use as a pressure sensitive adhesive [9], and as a viscosity modifying agent in drilling fluids [10]. The solid-state thermal, mechanical, and morphological properties were not probed.

In this study, a series of poly(I-*co*-NaSS) copolymers with varied molar ratios of isoprene to sodium styrene sulfonate was prepared using emulsion polymerization. The effect of ion-content on the morphology-property relationships of the ionomers is reported herein. This investigation into the effect of ionic sodium styrene sulfonate (NaSS)

* Corresponding author. Macromolecules Innovation Institute, Virginia Tech, Blacksburg, VA, 24061-0344, USA.
E-mail address: srturner@vt.edu (S.R. Turner).

https://doi.org/10.1016/j.polymer.2019.03.058
Received 5 September 2018; Received in revised form 22 March 2019; Accepted 24 March 2019
Available online 27 March 2019
0032-3861/

units copolymerized with isoprene yields fundamental structure-morphology-property information vital for compositional selection specific to material performance requirements.

2. Experimental

2.1. Materials

Sodium styrene sulfonate, cumene hydroperoxide, triethylenetetramine (TETA), Tween 80, 1-dodecanethiol, hydroquinone and 2,6-di-*t*-butyl-4-methyl phenol (DBMP) were purchased from Sigma Aldrich and used as received. Isoprene was obtained from Sigma Aldrich with *tert*-butylcatechol as an inhibitor. The monomer was stored at 5 °C, and prior to polymerization it was washed three times in a separatory funnel with 0.5 M NaOH followed by three washes with distilled water to eliminate the inhibitor [5]. After the washings, the isoprene was distilled at atmospheric pressure. Care was taken to have the final product collected in a flask partially submerged in an ice bath to avoid loss of isoprene, due to its high volatility. The sample was then sealed with a rubber stopper and purged with argon for 5 min with the flask partially submerged in an ice bath. The purified isoprene was either used immediately or stored at 5 °C until needed.

2.2. Synthesis of poly(I-co-NaSS)

An emulsion polymerization method presented by Siadat et al. [6], was adapted to prepare the poly(I-*co*-NaSS) series of polymers. Sodium pyrophosphate (0.3 g, 3.36×10^{-4} mol) and the desired amount of NaSS (1.0 g, 2.42 mmol) were added to a 250-mL round bottom flask and capped with a rubber septum. 60 mL of deaerated distilled water and TETA (0.5 g, 1.68×10^{-3} mol) were charged to the same flask via syringe, followed by a 5-min purge of argon gas. Into a separate 100-mL flask, Tween 80 (3.5 g, 1.31×10^{-3} mol), 14% dodecanethiol in toluene (0.43 g, 1.47×10^{-4} mol dodecanethiol) and cumene hydroperoxide (0.51 g, 1.68×10^{-3} mol) were added, and the flask was capped with a rubber septum. Isoprene (34.1 g, 0.25 mol) was added to the flask via syringe. The material from the 100-mL flask was then added to the 250-mL flask via syringe while running a purge of argon to maintain a constant pressure. The flask was placed in a water bath at room temperature and stirred for 22 h. A solution of 6 mL of methanol containing 0.048 g hydroquinone and 0.1 g DBMP was added to the flask and allowed to stir for 10 min. The milky white material was then transferred into 500 mL of methanol where it immediately began to coagulate. The solution was stirred for 24 h before being filtered with a Büchner funnel. The solid was added to 500 mL of DI water and stirred for 24 h before filtration. The polymer was dried overnight under vacuum at 50 °C. After removal from the oven the sample container was wrapped in foil, purged with argon and stored in the dark to prevent any photo-induced cross-linking. The nomenclature for the copolymers is poly(I-*co*-XX%NaSS), where XX is the measured molar percentage of NaSS in the copolymer.

2.3. Characterization

2.3.1. Chemical

A Varian Fourier-transform infrared spectroscopy (FTIR) instruemnt with a PIKE GladiATR attachment was used for infrared spectroscopy of the samples. The S═O stretching peak [6] at approximately 1200 cm^{-1} qualitatively shows the sulfur level in each copolymer. To quantitatively determine the concentration of sulfur in each copolymer, elemental analysis was conducted using combustion analysis performed by Atlantic Microlab Inc. Dynamic light scattering (DLS) was utilized to confirm ionic aggregation. All copolymer samples were dissolved at a concentration of 0.1 wt% copolymer in solvent. The co-solvent ratio for copolymers with NaSS concentrations less than 3.0 mol % was 95/5 v/v % toluene/1-butanol, while for copolymers with concentrations of NaSS greater than 3.0 mol % was 90/10 v/v% toluene/methanol. A co-solvent system was used in an attempt to optimize dissolution of the ionic and nonpolar components of the copolymers. The individual samples were sonicated in a glass vial for 1 min in a Branson 5800 Sonicator at 20 °C. The samples were then withdrawn using a glass syringe equipped with an 18-gauge needle and transferred through a 0.20 μm PTFE syringe filter to a quartz cuvette. The cuvette was then placed into the Malvern Zetasizer Nano Series DLS which measured the particle diameter of the samples at 25 °C. There was a 30 s equilibration time before three measurements were taken. Each measurement was the average of 10 scans that were each 10 s long. Intrinsic viscosity was measured using a Cannon-Fenske size 75 viscometer at 25 °C. Each copolymer was measured in solution at five different concentrations (0.10, 0.25, 0.50, 0.75, and 1.0 g/dL) using the same solvent as used for the DLS experiments. The inherent and reduced viscosities were plotted and the intrinsic viscosity was determined from the viscosity at zero concentration.

2.3.2. Film preparation

The solvents used for the preparation of films were the same as mentioned for DLS testing in the previous section. A solution of 5 wt% polymer in solvent was stirred overnight at room temperature. The viscous fluid was then poured into a polystyrene Petri dish containing a polytetrafluoroethylene (PTFE) liner (Welch Fluorocarbon). The film was allowed to air dry in a fume hood for 24 h, then dried in a vacuum oven at 50 °C overnight. This method produced a film of approximately 0.5 mm in thickness.

2.3.3. Thermal

Thermogravimetric analysis (TGA) was performed on a TA Q500 instrument using nitrogen as the purge gas, at a rate of 10 °C/min from ambient temperature to 600 °C. Differential scanning calorimetry (DSC) measurements were performed using a TA Q1000 DSC with nitrogen as the purge gas. The procedure utilized a "heat-cool-heat" series of cycles that involved heating from −80 °C to 190 °C at 5 °C/min, quench cooling back to −80 °C, then heating to 190 °C at 5 °C/min.

2.3.4. Mechanical

Dynamic mechanical analysis (DMA) temperature ramp experiments were performed using a TA Q800 DMA at a frequency of 1 Hz and a temperature ramp from −105 °C to 150 °C at 2 °C/min cooled with liquid nitrogen. Due to the affinity of polyisoprene to degrade at high temperatures, the ramp was not taken higher than 150 °C. To measure the stress/strain behavior, films were cut into dogbones measuring 32 mm × 2 mm x 0.5 mm (length x width x thickness). Stress relaxation tests were performed using 10 mm long samples on a TA Q800 DMA at 40 °C. The copolymers were taken to a strain of 50% and the stress relaxation was monitored for 1 h after deformation. A second set of stress relaxation tests were performed for the polymers containing 1.6 mol % and 4.6 mol % NaSS. When dissolving the copolymer, prior to casting, 5 wt % glycerol was added, and the film preparation and stress relaxation experiments were run under the same conditions. Tensile measurements were made at a strain rate of 30 mm/min on an Instron 5500 R. To measure hysteresis, the same Instron was utilized and the samples (with the same dimensions) were stretched to between 30 and 50% strain depending on the tensile properties of the copolymer. Each copolymer was taken to the maximum % strain achievable while still remaining in the initial linear region of the stress/strain curve (these strain percentages will be shown in the results and discussion section). The strain rate for all samples was 30 mm/min. Once the maximum strain was achieved, the strain was decreased to zero at a rate of 30 mm/min. One elongation (loading) and relaxation (unloading) counted as a cycle, and five cycles were performed. The percent hysteresis was calculated by taking the ratio of the area bounded by the loading-unloading curves to the total area under the loading curve [12].

2.3.5. Adhesion

Samples were dissolved in 15 wt % solution (concentrations of NaSS lower than 3.0 mol % used 95/5 v/v% toluene/1-butanol, while for polymers with concentrations of NaSS higher than 3.0 mol %, 90/10 v/v% toluene/methanol was used), doctor bladed at a thickness of 50 μm and a width of 1 in (24 mm) onto a sheet of mylar, then dried overnight under vacuum at 50 °C. The samples were adhered to steel plates by placing the adhesive side onto the plate and rolling a steel roller of approximately 2000 g over the Mylar twice. A 180° peel test was performed using a ChemInstruments Adhesion/Release Tester AR-1000 and pulled at a rate of 5 mm/s.

2.3.6. Small angle X-Ray scattering

Small angle x-ray scattering (SAXS) measurements were conducted using a Rigaku S-Max 3000 3 Pinhole SAXS system equipped with a rotating anode emitting x-rays with a wavelength of 0.154 nm (Cu K-α). The sample to detector distance was 1600 mm, and the q-range was calibrated using a silver behenate standard. Two dimensional SAXS patterns were obtained using a fully integrated 2D multiwire, proportional counting, gas-filled detector, with an exposure time of 2 h. All SAXS data were analyzed using the SAXSGUI software package to obtain radially integrated SAXS intensity versus scattering vector q, where $q = (4\pi/\lambda)\sin\theta$, θ is one half of the scattering angle and λ is the wavelength of the x-ray.

3. Results and discussion

3.1. Chemical composition of copolymer

The compositions of poly(I-*co*-NaSS) ionomers were characterized by FTIR, combustion elemental analysis, intrinsic viscosity, and DLS. ^{1}H nuclear magnetic resonance (NMR) spectroscopy did not yield quantitative results. Fig. S1 shows the qualitative IR results. The S═O bond absorbance at (1200 cm^{-1}) [13] increases as NaSS content increases. Combustion sulfur analysis was performed to quantitatively confirm NaSS content. As shown in Table 1, NaSS content of prepared copolymers ranged from 0 to 4.6 mol%. The error associated with elemental analysis is approximately ± 0.3% of the measured value, allowing accurate comonomer content determination at the low sulfonate concentrations investigated. IR and elemental analysis data confirm that the incorporated concentration of NaSS increased as the feed concentration of NaSS increased.

Molecular weight could not be determined via size exclusion chromatography due to aggregates remaining in solution as confirmed by DLS. An approximation of the molecular weight was determined by intrinsic viscosity measurements using the Mark-Houwink-Sakurada (MHS) equation [14] where [η] is the intrinsic viscosity, K and α are the MHS parameters measured in toluene and M_v is the viscosity molecular weight:

$$[\eta] = KM_v^{\alpha}$$

Homopolymerized polyisoprene can contain several stereochemistries including *cis*-1,4-, *trans*-1,4-, 1,2-, and 3,4-polyisoprene, with each isomer leading to different K and α values. Free radical emulsion polymerized polyisoprene has a distribution of isomers as follows: 24.4% *cis*-1,4, 62.0% *trans*-1,4, 6.1% 1,2, and 7.5% 3,4 [15]. K and α values have been measured for 100% *trans*-1,4-poyisoprene [14] and for 70% *cis*-1,4, 23% *trans*-1,4 and 7% 3,4-polyisoprene [16]. The viscosity results for the copolymers with lower amounts of NaSS are shown in Table 2, utilizing the K and α values from references 14 and 16. These values are an approximation of the molecular weights, due to the evidence of aggregates in the polymer solution. Notably all of the molecular weights were high, in the range of 200,000 to 300,000 g/mol. The molecular weight increase correlation with ion concentration increase could be due to an increase in molecular weight, chemical crosslinking, or an increase in the dissolution of the polymer as the ion content increases. The copolymers containing above 3.0 mol % of NaSS could not be measured, due to the lack of solubility observed by the swollen gel in solution, thus creating an inability to flow consistently through the capillary viscometer.

DLS was used to probe aggregate structure in dispersed poly(I-*co*-NaSS) copolymers. Copolymers containing 1.2 mol % and 1.6 mol % of NaSS flowed easily through a 0.20 μm PTFE filter, however, the copolymers of higher NaSS content contained aggregates on a size scale sufficient to compromise filtration. For the two copolymer compositions that were successfully filtered, the correlation data showed evidence of large aggregates with high polydispersity (Figs. S2 and S3). The DLS trace for both copolymers were multimodal, suggesting the existence of aggregates that could be attributed to high molecular weight or chemical crosslinking.

3.2. Mechanical properties

Table 3 and Fig. 1 show the stress-strain behavior of the poly(I-*co*-NaSS) copolymers. Increasing NaSS content increases the stress and strain at break. For ion contents less than 3.4 mol % the stress and strain at break are indicative of uncrosslinked elastomers, however, for the copolymers with ion contents greater than 3.4 mol % these properties increased significantly. The behavior shown in the tensile traces is an indication of a systematic increase in electrostatic interactions within the copolymers as the ion concentration is increased.

The storage moduli of the polymers are shown in Fig. 2. After the decrease in moduli at around −40 °C, all of the polymers show a plateau indicating the inability to flow. The storage modulus increased with increasing ion content in the rubber plateau, indicating an increase in stiffness and, potentially, an increase in the concentration of physical crosslinks. According to the theory of rubber elasticity the modulus should increase as temperature increases [17]. Fig. 2 shows either steady behavior or a slight decrease in the modulus with temperature, which indicates that there is likely physical interactions happening within the copolymer that prevents this expected increase in modulus. The copolymers were taken up to 220 °C to probe for potential phase separation between polar and nonpolar segments in the ionomer [18], but there was no evidence of this behavior.

The thermal properties of the polymers were tested to better understand the morphological changes as ion concentration increases. The data in Table 4 shows that the glass transition temperatures (T_g) measured by both DSC and DMA (Fig. 2) are not affected by ion content. It is reasonable to assume for all of the copolymers that the low incorporation of NaSS would not significantly affect the Tg of

Table 1
Compositions of a series of poly(I-*co*-NaSS) with increasing concentrations of NaSS obtained from elemental analysis compared to the theoretical values.

Copolymers	Theoretical weight % sulfur	Measured weight % sulfur	Theoretical mol % NaSS	Measured mol% NaSS
polyisoprene	0.0	0.0	0.0	0.0
poly(I-*co*-1.2NaSS)	0.15	0.18	0.96	1.2
poly(I-*co*-1.6NaSS)	0.30	0.25	1.9	1.6
poly(I-*co*-2.6NaSS)	0.44	0.41	2.8	2.6
poly(I-*co*-3.4NaSS)	0.61	0.53	3.9	3.4
poly(I-*co*-4.6NaSS)	0.72	0.73	4.6	4.6

Table 2
Intrinsic viscosity and approximate molecular weights for poly(I-*co*-NaSS) polymers. (a) [14] uses *K* and *α* values of 1.76×10^{-4} dl/g and 0.73 for 100% *trans*-1,4-polyisoprene, and (b) [16] using *K* and *α* values of 1.72×10^{-4} dl/g and 0.74 for 70% *cis*-1,4, 23% *trans*-1,4 and 7% 3,4-polyisoprene.

Copolymers	Intrinsic viscosity (dl/g)	Approximate Molecular Weight (M_v) (g/mol)[a]	Approximate Molecular Weight (M_v) (g/mol)[b]
poly(I-*co*-1.2NaSS)	1.29	197,000	172,000
poly(I-*co*-1.6NaSS)	1.50	242,000	211,000
poly(I-*co*-2.6NaSS)	2.05	371,000	322,000
poly(I-*co*-3.4NaSS)	Due to incomplete dissolution, the samples could not be measured		
poly(I-*co*-4.6NaSS)			

Table 3
Tensile results for poly(I-*co*-NaSS) copolymers.

Polymer	Young's Modulus (MPa)	Stress at break (MPa)	Strain at break (%)
poly(I-*co*-1.2NaSS)	4.5 ± 0.2	0.16 ± 0.10	590 ± 60
poly(I-*co*-1.6NaSS)	5.8 ± 0.3	0.32 ± 0.10	850 ± 90
poly(I-*co*-2.6NaSS)	5.4 ± 0.1	0.60 ± 0.30	1300 ± 100
poly(I-*co*-3.4NaSS)	9.2 ± 0.4	2.1 ± 0.7	2110 ± 80
poly(I-*co*-4.6NaSS)	8.9 ± 0.2	2.3 ± 4.0	2200 ± 100

polyisoprene. If well-defined ionic aggregation was present, a systematic shift in the T_g would be expected.

The T_g results from DSC confirm the polyisoprene isomer present. The T_g of *cis*-1,4-polyisoprene is approximately −73 °C, while the T_g of *trans*-1,4-polyisoprene is −58 °C as measured by DSC [19]. The T_g of the copolymers was −60 ± 4 °C, indicating that the copolymers contain more of the *trans*-1,4 isoprene isomer. Also of note is the fact that the DMA tan delta value is approximately 20 °C higher than the T_g measured by DSC, due to the differing testing methods (e.g. measuring frequency instead of heat flow) [20].

Uncrosslinked polyisoprene can drop to a modulus close to zero strain at approximately 30 s [21] in stress relaxation conditions similar to those utilized in this work. The results for the poly(I-*co*-NaSS) series in (Fig. 3) show that as the ion content increases, the copolymers tend to maintain a higher stress over time at 50% strain. Poly(I-*co*-1.2NaSS) and poly(I-*co*-1.6NaSS) show a reduction in sustained stress, but still at higher stress levels than the high molecular weight homopolymerized polyisoprene studied by Fuller and Fulton [21]. The copolymer samples containing between 2.6 and 4.6 mol % NaSS show a much lower reduction in deformation of the samples over time. Poly(I-*co*-1.6NaSS) and poly(I-*co*-4.6NaSS) were dissolved in 5 wt% glycerol, along with the usual toluene-butanol mixture. As seen in Fig. 4 both copolymers showed a slight drop in the stress level with the addition of glycerol, which acts as a plasticizer that will inhibit the physical interactions in the copolymer. If the copolymers were only physically crosslinked, the stress should quickly relax to zero, as is the case for homopolymerized polyisoprene. In the absence of this relaxation to zero, it can be determined that there is covalent crosslinking in the system. The slight drop in stress does indicate a presence of some physical crosslinking, (as also shown in the tensile and DMA results, Figs. 1 and 2).

To determine the ability of the copolymers to respond to a load, hysteresis was measured. Table 5 shows the hysteresis results for each copolymer in the linear region of the stress-strain curve. In terms of % hysteresis, all of the copolymer compositions were within approximately 7% hysteresis. There was evidence of a slight decrease in percent hysteresis with increasing ion content, however there is a slight increase in percent hysteresis for the copolymer with the highest ion concentration. This indicates that the ion concentration does not have much of an impact on the initial increase in strain and recovery from that strain. This is likely due to the fact that the copolymer chains haven't been sufficiently stretched to allow the ions to come into contact with each other. Future work should include investigating hysteresis at higher strains.

3.2.1. Adhesion peel testing

The adhesion of the copolymers to steel was measured in 180° peel tests (Fig. 5). During the peel test, the copolymers failed mostly

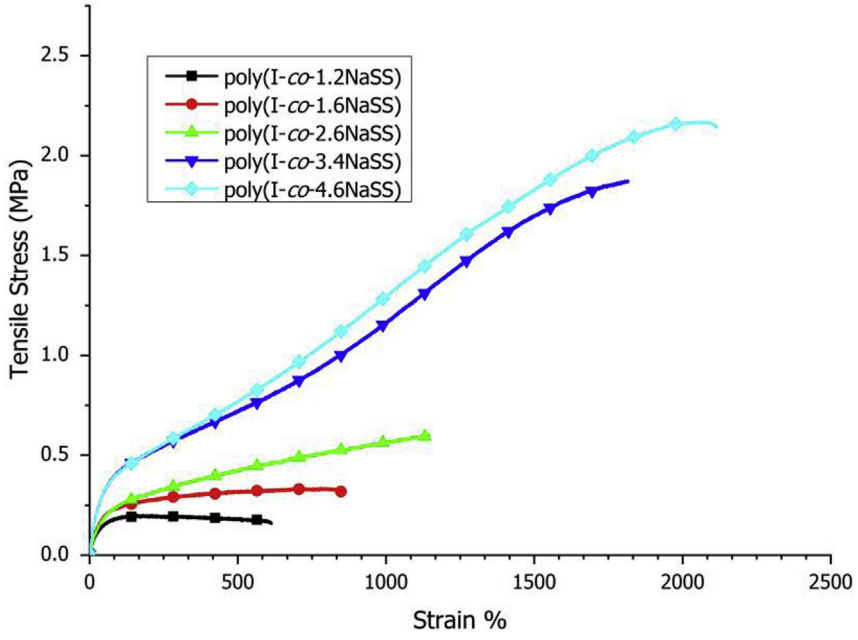

Fig. 1. Stress vs strain behavior for a series of poly(I-*co*-NaSS) samples.

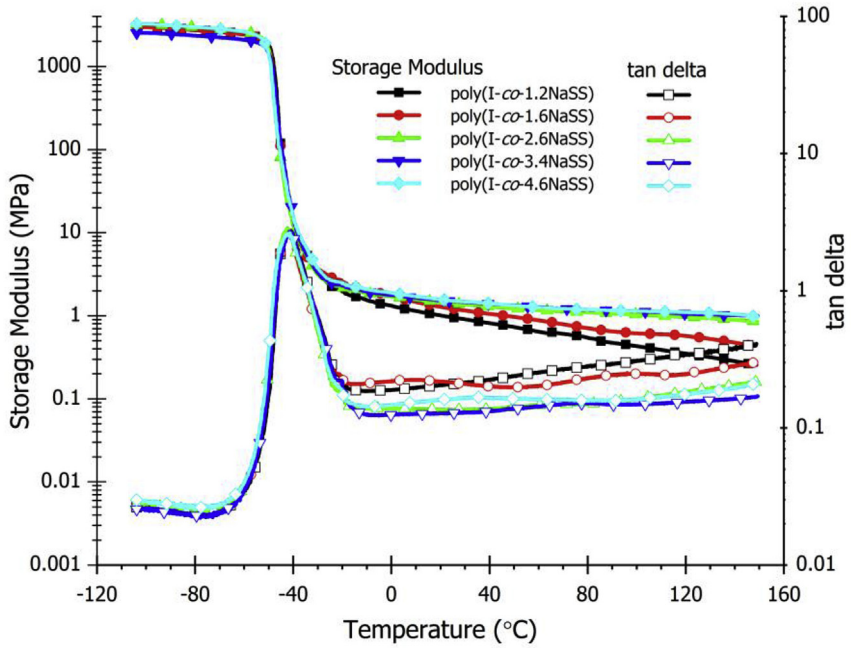

Fig. 2. Storage moduli from DMA for a series of poly(I-*co*-NaSS).

Table 4
T_g determined by DSC, and tan delta determined by DMA.

Copolymer	T_g (°C)	tan delta (°C)
poly(I-*co*-1.2NaSS)	−62.1	−42.1
poly(I-*co*-1.6NaSS)	−60.8	−41.1
poly(I-*co*-2.6NaSS)	−61.7	−41.1
poly(I-*co*-3.4NaSS)	−60.7	−41.2
poly(I-*co*-4.6NaSS)	−61.1	−41.4

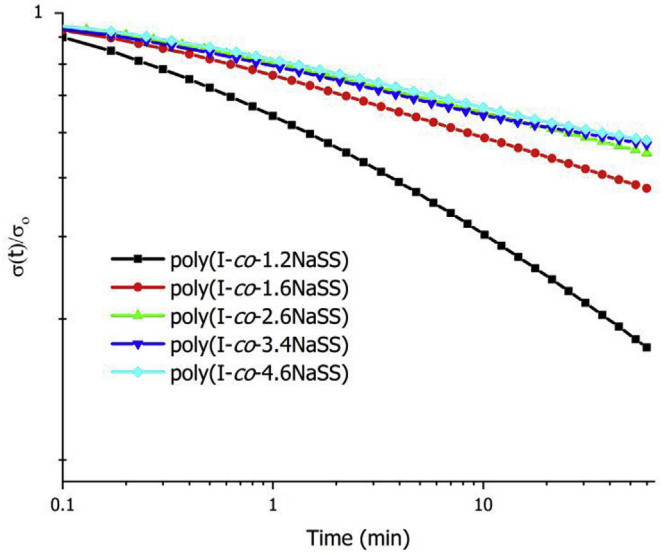

Fig. 3. Stress relaxation behavior for a series of poly(I-*co*-NaSS) samples at 50% strain.

adhesively, but in some samples (in all of the different compositions), there was both adhesive and cohesive failure. Peel strength increased significantly with increasing ion content, due to the increase in adhesive strength from electrostatic interactions.

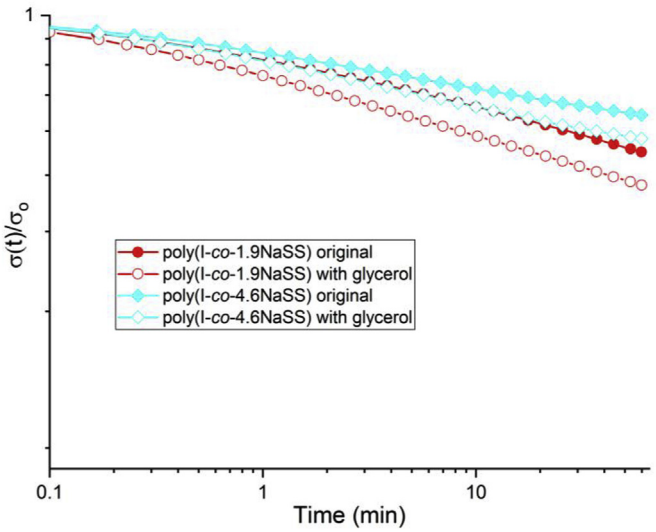

Fig. 4. Stress relaxation behavior of poly(I-*co*-1.9NaSS) and poly(I-*co*-4.6NaSS) with and without the addition of 5 wt % glycerol.

Table 5
Hysteresis results for poly(I-*co*-NaSS) samples.

Copolymer	Maximum strain (%)	% Hysteresis First Cycle	Avg. % Hysteresis Second-Fifth Cycles
poly(I-*co*-1.2NaSS)	25	29.0	27.8 ± 0.4
poly(I-*co*-1.6NaSS)	30	25.5	23.8 ± 0.3
poly(I-*co*-2.6NaSS)	30	23.0	21.2 ± 0.2
poly(I-*co*-3.4NaSS)	40	21.7	19.2 ± 0.1
poly(I-*co*-4.6NaSS)	40	24.6	22.2 ± 0.2

3.3. Morphology

Small angle X-ray scattering (SAXS) was utilized to probe the morphology of the series of poly(I-*co*-NaSS) copolymers. The presence of free ions, if distributed randomly in the matrix domain of the polymer would increase the overall electron density of the matrix, thus

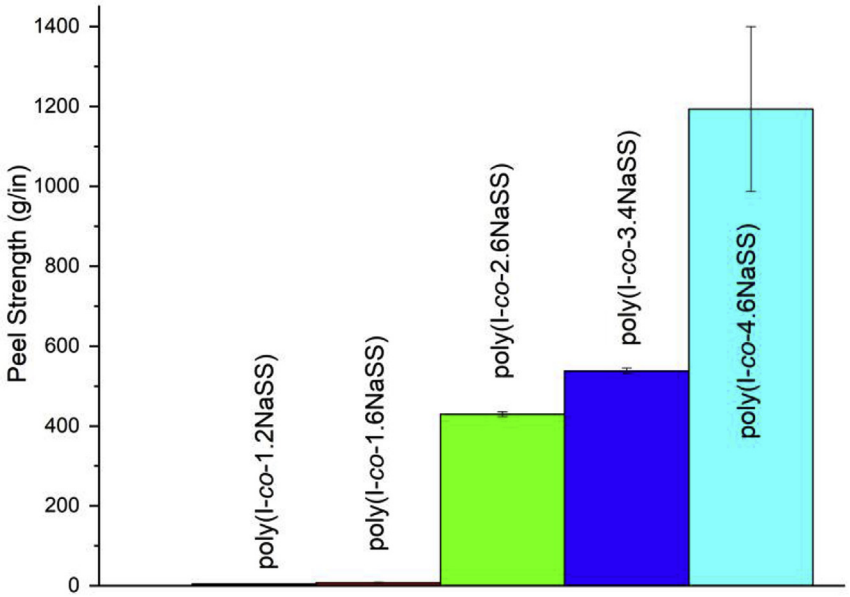

Fig. 5. 180° Peel Test data for poly(I-*co*-SS) samples.

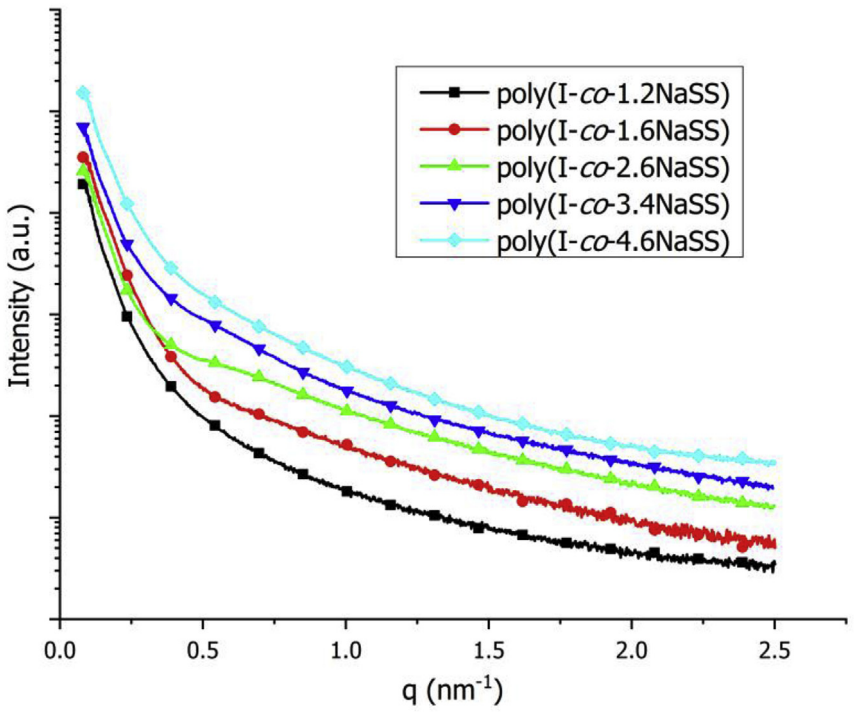

Fig. 6. Vertically shifted SAXS results for poly(I-*co*-NaSS) copolymers.

decreasing the contrast between the ionic and nonpolar domains [22]. Turner et al. hypothesized that lightly sulfonated polystyrene ionomers prepared by emulsion copolymerization would contain small blocks of 3–4 NaSS repeat units randomly distributed along the backbone [23], indicating that it could be possible to see a decrease in overall contrast between the two phases in this system [24]. Typically, the characteristic ionomer peak for sulfonated polystyrene lies at q values in the range of 1.5–2.5 nm^{-1} [25,26]. Fig. 6 shows the scattering curves obtained from SAXS for the series of poly(I-*co*-NaSS) copolymers. The scattering profile for poly(I-*co*-1.2NaSS) is featureless, suggesting the copolymer does not exhibit well-ordered ionic aggregation. Although excess scattering in the vicinity of $q = 0.7\ nm^{-1}$ is present in the higher ion-content polymers, these shoulders are broad and likely attributed to compositional inhomogeneities present in chemically crosslinked polymers. Unlike polystyrene based ionomers there is no evidence of large-scale ionic aggregation or of a well-defined multiplet structure in this series of poly(I-*co*-NaSS).

Following the hypothesis presented by Turner et al. [23], the behavior of the monomers during polymerization can be postulated: When the emulsion polymerization begins, the NaSS monomer is present in the aqueous phase, while the isoprene monomer is in a separate, nonaqueous phase. Upon initiation, the NaSS will begin polymerizing with other NaSS monomers in the aqueous phase prior to introduction into the non-aqueous phase and subsequent co-polymerization with the isoprene monomers. This leads to short blocks of NaSS randomly distributed throughout the isoprene backbone. One hypothesis for the

observed mechanical properties (specifically the increase in stress and strain at break, along with the stress relaxation performed with glycerol) of the system is that it is covalently crosslinked as well as physically crosslinked. In the presence of covalent crosslinks, the small blocks of NaSS could be restricted within the network preventing large-scale aggregation of ions. Covalent crosslinking would necessarily give rise to the presence of ionic doublets and triplets (rather than multiplets) suggested by the tensile and stress-relaxation results, while also explaining the absence of a characteristic ionic aggregate peak in scattering profiles obtained by SAXS.

4. Conclusions

Although well-defined ionic aggregation was not observed using SAXS, the tensile and stress-relaxation data suggest that small-scale electrostatic interactions, that are bound by covalent crosslinks, are responsible for the mechanical properties of the poly(I-*co*-NaSS) copolymers. This is manifested uniformly in the tensile, stress relaxation and adhesion properties. The present study provides fundamental inter-relationships between chemical structure, morphology and physical behavior.

Conflicts of interest

The authors declare no conflict of interest.

Acknowledgements

This material is based upon work supported by the National Science Foundation under Grant No. DMR-1507245 and Grant No. DMR-0923107. The authors would like to thank the Virginia Tech Chemistry Department and Macromolecules Innovation Institute as well as Dr. Timothy E. Long for instrument use.

Appendix A. Supplementary data

Supplementary data to this article can be found online at https://doi.org/10.1016/j.polymer.2019.03.058.

References

[1] R.D. Lundberg, Elastomers and fluid applications, in: M.R. Tant, K.A. Mauritz, G.L. Wilkes (Eds.), Ionomers Synth. Struct. Prop. Appl, Chapman & Hall, New York City, NY, 1997, pp. 477–501.
[2] A. Eisenberg, B. Hird, R.B. Moore, A new multiplet-cluster model for the morphology of random ionomers, Macromolecules 23 (1990) 4098–4107.
[3] R.D. Lundberg, H.S. Makowski, A comparison of sulfonate and carboxylate ionomers, in: A. Eisenberg (Ed.), Ions Polym, first ed., American Chemical Society, Washington DC, 1980, pp. 21–36.
[4] M.R. Tant, G.L. Wilkes, Structure and properties of hydrocarbon-based ionomers, in: M.R. Tant, K.A. Mauritz, G.L. Wilkes (Eds.), Ionomers Synth. Struct. Prop. Appl, first ed., Chapman & Hall, New York City, NY, 1997, pp. 261–289.
[5] B. Siadat, B. Oster, R.W. Lenz, Preparation of ion-containing elastomers by emulsion copolymerization of dienes with olefinic sulfonic acid salts, J. Appl. Polym. Sci. 26 (1981) 1027–1037.
[6] B. Siadat, R.W. Lenz, Preparation of esters of styrene sulfonic acid and their emulsion copolymerization with isoprene, J. Polym. Sci. 18 (1980) 3273–3287.
[7] P.K. Agarwal, S.R. Turner, R.D. Lundberg, M.L. Evans, Emulsion type Adhesive compositions, 483,960, U.S. Patent 4 (November, 20, 1984) (n.d).
[8] P.K. Agarwal, R.D. Lundberg, J. Wagensomer, F.C. Jagisch, Emulsion type Adhesive compositions, 517,250, U.S. Patent 4 (May 14, 1985) (n.d).
[9] P.K. Agarwal, T. Pugel, Novel pressure sensitive adhesive compositions (C-2511), 066,694, U.S. Patent 5 (November, 19, 1991) (n.d).
[10] S.R. Turner, R.D. Lundberg, T.O. Walker, Drilling fluids based on sulfonated elastomeric polymers, 425,462, U.S. Patent 4 (January 10, 1984) (n.d).
[11] B. Siadat, R.D. Lundberg, R.W. Lenz, Solubility behavior of copolymers of isoprene and sodium styrenesulfonate, Macromolecules 14 (1981) 773–776.
[12] R.A. Nallicheri, M.F. Rubner, Influence of cross-linking on the hysteresis behavior of poly(urethane-diacetylene) segmented copolymers, Macromolecules 24 (1991) 526–529.
[13] R.M. Silverstein, F.X. Webster, D.J. Kiemle, Spectrometric Identification of Organic Compounds, Seventh, John Wiley & Sons, Inc., New York City, NY, 2005.
[14] P.N. Chaturvedi, K. Patel, Dilute-solution properties of trans-l,4-polyisoprene, J. Polym. Sci. Polym. Phys. Ed 23 (1985) 1255–1262.
[15] M.J. Hackathorn, M.J. Brock, Polyisoprene Structure from thermal degradation data, Polym. Lett. 8 (1970) 617–625.
[16] N. Hadjichristidis, J.E.L. Roovers, Synthesis and solution properties of linear , four-branched , and six-branched star polyisoprenes, J. Polym. Sci. Polym. Phys. Ed 12 (1974) 2521–2533.
[17] C. Price, Thremodynamics of rubber elasticity, Proc. R. Soc. A. 351 (1976) 331–350.
[18] R.A. Weiss, J.J. Fitzgerald, D. Kim, Viscoelastic behavior of lightly sulfonated polystyrene ionomers, Macromolecules 24 (1991) 1071–1076, https://doi.org/10.1021/ma00005a015.
[19] J. Brandup, E.A. Immergut, Polymer Handbook, fourth ed., Wiley-Interscience, New York City, NY, 1999.
[20] B. Wunderlich, Thermal Analysis of Polymeric Materials, Springer, New York City, NY, 2005.
[21] K.N.G. Fuller, W.S. Fulton, The influence of molecular weight distribution and branching on the relaxation behaviour of uncrosslinked natural rubber, Polymer 31 (1990) 609–615, https://doi.org/10.1016/0032-3861(90)90276-5.
[22] L.N. Venkateshwaran, M.R. Tant, G.L. Wilkes, P. Charlier, R. Jerome, Structure-property comparison of sulfonated and carboxylated telechelic ionomers based on polyisoprene, Macromolecules 25 (1992) 3996–4001.
[23] S.R. Turner, R.A. Weiss, R.D. Lundberg, The emulsion copolymerization of styrene and sodium styrene sulfonate, J. Polym. Sci. Polym. Chem. Ed. 23 (1985) 535–548.
[24] L.J. Anderson, X. Yuan, G.B. Fahs, R.B. Moore, Blocky ionomers via sulfonation of poly(ether ether ketone) in the semicrystalline gel state, Macromolecules 51 (2018) 6226–6237, https://doi.org/10.1021/acs.macromol.8b01152.
[25] D.J. Yarusso, S.L. Cooper, Microstructure of ionomers: interpretation of small-angle x-ray scattering data, Macromolecules 16 (1983) 1871–1880, https://doi.org/10.1021/ma00246a013.
[26] D.J. Yarusso, S.L. Cooper, Analysis of SAXS data from ionomer systems, Polymer 26 (1985) 371–378, https://doi.org/10.1016/0032-3861(85)90196-X.